

## Luminescence and Raman Spectra of Acetylacetone at Low Temperatures

Vlasta Mohaček-Grošev<sup>a</sup>, Krešimir Furić<sup>a</sup>, Hroje Ivanković<sup>b</sup>

### Abstract

Raman spectra of acetylacetone were recorded for molecules isolated in an argon matrix at 10 K and for a polycrystalline sample. In the solid sample, broad bands appear superimposed on a much weaker Raman spectrum corresponding mainly to the stable enol form. The position of these bands depends on the excitation wavelength (514.5 and 488.8 nm argon ion laser lines were used), sample temperature, and cooling history. They are attributed to transitions from an excited electronic state to various isomer states in the ground electronic state. Laser photons have energies comparable to energies of a number of excited triplet states predicted for a free acetylacetone molecule (Chen, X.-B.; Fang, W.-H.; Phillips, D. L. *J. Phys. Chem. A* **2006**, *110*, 4434). Since singlet-to-triplet photon absorption transitions are forbidden, states existing in the solid have mixed singlet/triplet character. Their decay results in population of different isomer states, which except for the lowest isomers SYN enol, TS2 enol (described in Matanović I.; Došlić, N. *J. Phys. Chem. A* **2005**, *109*, 4185), and the keto form, which can be detected in the Raman spectra of the solid, are not vibrationally resolved. Differential scanning calorimetry detected two signals upon cooling of acetylacetone, one at 229 K and one at 217 K, while upon heating, they appear at 254 and 225 K. The phase change at higher temperature is attributed to a freezing/melting transition, while the one at lower temperature seems to correspond to freezing/melting of keto domains, as suggested by Johnson et al. (Johnson, M. R.; Jones, N. H.; Geis, A; Horsewill, A. J.; Trommsdorff, H. P. *J. Chem. Phys.* **2002**, *116*, 5694). Using matrix isolation in argon, the vibrational spectrum of acetylacetone at 10 K was recorded. Strong bands at 1602 and 1629 cm<sup>-1</sup> are assigned as the SYN enol bands, while a weaker underlying band at 1687 cm<sup>-1</sup> and a medium shoulder at 1617 cm<sup>-1</sup> are assigned as TS2 enol bands.

### Introduction

Acetylacetone (2,4-pentanedione), acac, serves as a model for the study of intramolecular hydrogen bonding, together with other  $\beta$  diketone molecules.<sup>1</sup> It is often used as a complexing agent with various metal ions<sup>2,3</sup> and in producing compounds for organic light-emitting diodes.<sup>4</sup> It is a rather small molecule but of rich dynamics, exhibiting effects of tautomerism. In the simplest model, two molecular species, enol and keto, exist in equilibrium at room temperature in the approximate ratio of 3:1 in favor of the enol.<sup>1</sup> Temperature<sup>5</sup> and solvents<sup>6</sup> are known to affect this ratio and move it either toward the enol or keto side.

---

<sup>a</sup> Ruđer Bošković Institute, P.O. Box 180, Bijenička c. 54, 10002 Zagreb, Croatia (mohacek@irb.hr)

<sup>b</sup> Faculty of Chemical Engineering and Technology, Marulićev trg 19, 10000 Zagreb, Croatia

The potential energy surface that determines the positions of the tautomeric minima has been intensively studied.<sup>7-18</sup> Matanović et al. explored the potential energy surface for proton transfer in acetylacetone.<sup>12</sup> The ground state was found to be SYN enol (see Figure 1). The transition state TS2 was only 0.25 kcal/mol higher in energy than SYN enol, and the transition state TS1 had an energy that was 1.45 kcal/mol higher than that of SYN. The main difference in geometry between the TS1 and TS2 transition states concerns the orientation of the methyl groups (Figure 1). Although the SYN, TS1, and TS2 conformers have  $C_s$  symmetry, the experimental difficulties in detecting the position of the hydroxyl proton raise the possibility of identifying unrelaxed molecules in the TS1 and TS2 states and reporting them as molecules having  $C_{2v}$  symmetry because the methyl groups are placed symmetrically with respect to the plane containing oxygen atoms in both TS1 and TS2. Thus, the X-ray diffraction experiment conducted at 210 and 110 K by Boese et al.<sup>19</sup> reported acetylacetone molecules with  $C_{2v}$  symmetry. Johnson et al.<sup>20</sup> measured methyl tunneling splitting energies in polycrystalline acac using the quasielastic neutron scattering diffraction technique. They showed that rapid cooling of liquid acac results in a polycrystalline mixture of enolic and keto tautomers and succeeded in producing pure enolic polycrystalline powder. The method used was to anneal the sample below the melting point (at 245 K) for 10 h. The two different methyl tunneling splitting energies that were measured for the annealed sample at 5 K were assigned as originating from two different methyl groups of the same molecule. Their work supports the SYN enol form as the stable enolic form of acetylacetone in the crystal state.

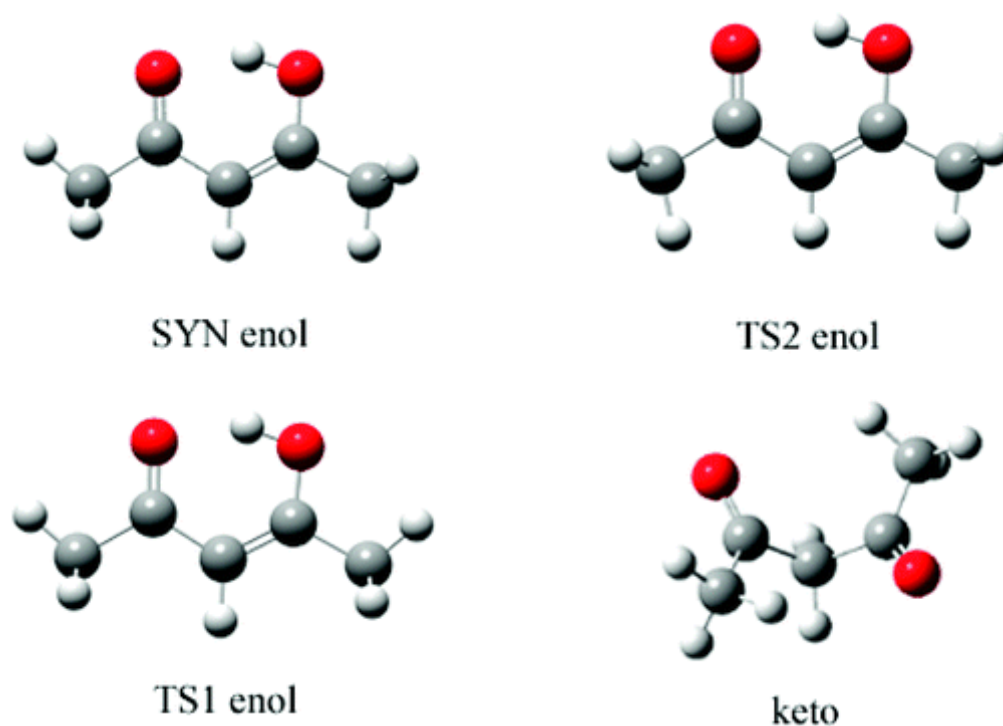


**Fig 1** Figure 1 Enol (SYN, TS2, and TS1) and keto tautomers of acetylacetone. The SYN enol is the most stable configuration, and TS2 and TS1 are transition states 0.25 and 1.45 kcal/mol higher in energy than SYN, respectively.<sup>10</sup>

For the free acac molecule, experiments involved in determination of the minimum energy conformation include high-resolution rotational spectra of Caminati and Grabow<sup>21</sup> and electron diffraction experiments by Lowrey et al.,<sup>22</sup> which were in favor of the  $C_{2v}$  equilibrium structure. On the contrary, electron diffraction experiments by Ijima et al.<sup>23</sup> and Srinivasan et al.<sup>24</sup> argued that the planar but nonsymmetrical  $C_s$  structure was the most stable. Camerman et al. identified enolic acetylacetone as residual solvent in a crystal of antiepileptic drugs.<sup>25</sup>

After the discovery of Veierov et al.<sup>26</sup> that acetylacetone displays isomerization upon UV illumination, a number of studies were devoted to isolation of different isomers and calculation of their relative energies.<sup>27-34</sup>

Vibrational studies of acetylacetone gave a thorough assignment of bands for the enolic  $C_s$  tautomer, and some, more intense, bands of the keto tautomer could be confidently attributed.<sup>35-</sup>

<sup>39</sup> Tayyari<sup>35</sup> reported the SYN conformer as the most stable form (his notation **I**), which coexists in liquid with TS2 (**II** in his notation). He assigned the low-temperature  $1635\text{ cm}^{-1}$  band to the stable conformer and the  $1600\text{ cm}^{-1}$  low-temperature band to the conformer **II** (TS2). Chiavassa et al. first performed infrared matrix-isolation experiments,<sup>36</sup> and later Coussan et al. included induced UV and IR isomerizations of matrix-isolated acac.<sup>29</sup>

We undertook the Raman matrix-isolation experiment to verify the conclusion of Cohen and Weiss<sup>5</sup> and Tayyari<sup>35</sup> that there exists two enolic forms rapidly interconverting in the liquid. Also, low-temperature Raman spectra of the polycrystalline sample were collected from 10 to 300 K for the study of the possible disorder of the methyl groups.

## Experimental Methods

Acetylacetone (acac), 99.5% pure, was purchased from Sigma-Aldrich (Fluka) and transferred to a capillary tube with several freeze–pump–thaw cycles performed to eliminate dissolved air. The capillary was sealed under vacuum. For low-temperature measurements, we used several cryostats, an old CTI model 21 CRYOGENICS, a new CCS350 JANIS RESEARCH, both with a closed cycle of liquid helium, which could reach 10 K, and a VPF 700 from JANIS RESEARCH, operating with liquid nitrogen for temperatures as low as 80 K. For temperature control, a Lake Shore 331 instrument was used.

For the matrix-isolation experiment, a small amount of pure liquid acac was transferred into glass vial, and freeze–pump–thaw cycles were repeated. The vial with frozen sample was evacuated with rotary and diffusion pumps and then connected to a Swagelok needle valve leading to the cold golden-plated cryostat finger on one side and to the reservoir of argon on the other. The vapor pressure of liquid acac is 0.8 kPa (from the Sigma-Aldrich website). After the sample melted at room temperature, acac vapor was allowed to mix with argon from the reservoir held at a pressure of 1 atm by opening the valve toward argon. The matrix ratio was estimated from the ratio of pressures of acetylacetone vapor and argon and was approximately 1:100. The vapor/gas mixture was deposited on the golden surface inside of the cryostat head

cooled to 10 K. Traces of air were found ( $2328\text{ cm}^{-1}$  from the  $\text{N}_2$  stretching band and  $1554\text{ cm}^{-1}$  from the  $\text{O}_2$  stretching band) because of imperfect sealing.

A differential scanning calorimetry experiment was performed with Netzsch DSC 200 instrument equipped with a liquid nitrogen cooling system in a He atmosphere. The cooling rate was 5 K/min, and the heating rate was also 5 K/min.

Raman spectra were recorded with the DILOR Z24 Raman spectrometer, while excitation was provided with an argon ion laser (COHERENT INNOVA 400) operating at 514.5 and 488.8 nm with a laser power of 200 mW at the sample. Spectra were recorded in the sequential mode, and the step sizes used ranged from 0.5 to  $4\text{ cm}^{-1}$ . The slit width was  $300\text{ }\mu\text{m}$ , giving spectral resolution of  $2.3\text{ cm}^{-1}$ .

## Results

**Matrix-Isolation Experiment.** Infrared and Raman spectra of liquid acac are shown in Figure 2, and Raman spectrum of the matrix-isolated sample is shown in Figure 3. The positions of selected observed bands are listed in Table 1, while the complete list is given in the Supporting Material. The assignment of the enol bands was done according to the calculation by Matanović and Došlić,<sup>7</sup> and the keto bands attributed according to our calculation performed at the B3LYP/6-311++G(d, p) level of theory.<sup>40</sup> The calculated unscaled values for the keto tautomer are listed in Table 2 of the Supporting Material. Several keto bands in liquid could be confidently identified by comparing the spectra of polycrystalline acac containing only enol molecules and the liquid spectra; the  $1730\text{ cm}^{-1}$  band was attributed to  $\text{C}=\text{O}$  groups stretching out of phase, the  $1709\text{ cm}^{-1}$  band was attributed to  $\text{C}=\text{O}$  groups stretching in phase, the  $1157\text{ cm}^{-1}$  band corresponded to the  $\delta(\text{CH}_2)$ , the  $957\text{ cm}^{-1}$  band corresponded to skeletal  $\text{C}-\text{C}$  stretching, the  $621\text{ cm}^{-1}$  band was assigned to  $\text{C}-\text{CH}_2-\text{C}$  bending, and the  $330\text{ cm}^{-1}$  band was assigned to  $\text{H}_3\text{C}-\text{C}-\text{C}$  bending.

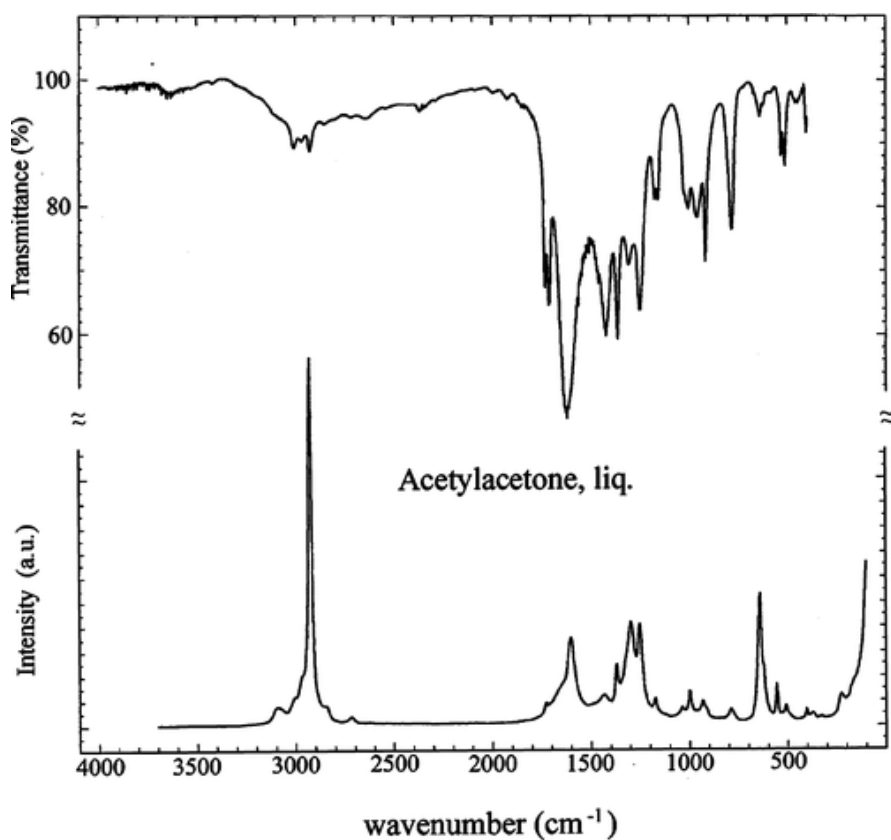


Fig 2 Infrared and Raman spectra of liquid acetylacetone.

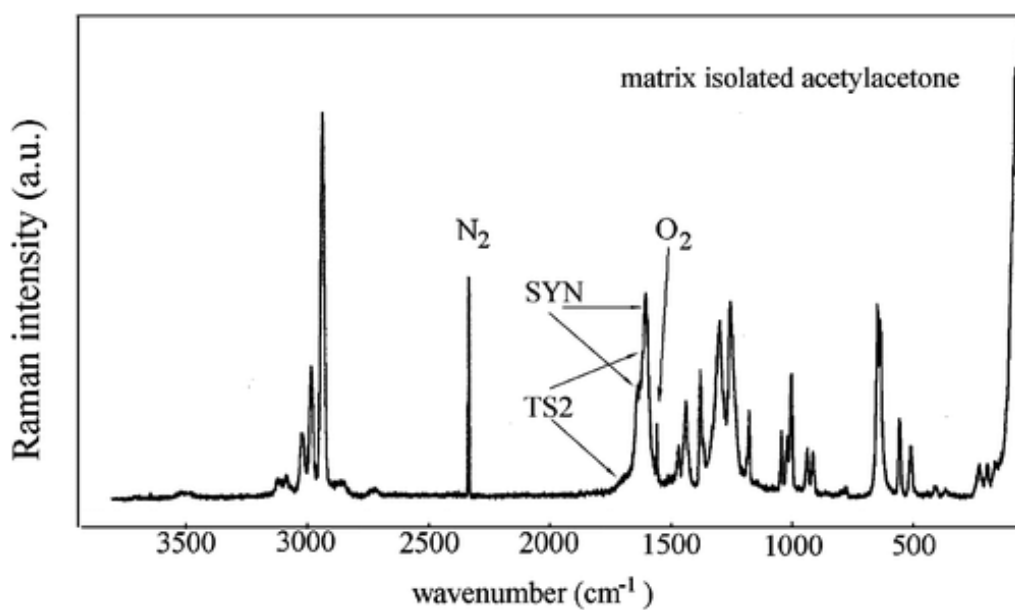


Fig 3 Raman spectrum of acetylacetone isolated in an argon matrix at 10 K (10–3800 cm<sup>-1</sup>). The matrix ratio is ~1:100.

Mohaček-Grošev, V., Furić, K., Ivanković, H. (2007), "Luminescence and Raman Spectra of Acetylacetone at Low Temperatures", *Journal of Physical Chemistry. A*, Vol. 111, No. 26, pp. 5820-5827.

Table 1 Selected Observed Raman and Infrared Bands of Acetylacetone (cm<sup>-1</sup>)<sup>a,b</sup>

Raman matrix 10 K	Raman solid 10 K enols + keto	Raman solid 10 K enols + keto	Raman solid 10 K enols	Raman liquid 295 K enols + keto	infrared liquid 295 K enols + keto	assignment
	<b>1800 m, vbr</b>					luminescent band
	1715 w	1715 vvw		1732 w	1730 s	$\nu(\text{C}=\text{O})$ keto, out-of-phase
	1700 w	1698 vvw			1709 s	$\nu(\text{C}=\text{O})$ keto, in-phase
1687 w,sh			1683 w			$\nu(\text{C}=\text{C}-\text{C}=\text{O})$ TS2 enol
				1672 br, =sh		
	1651 mw,sh	1653 mw,sh	1652 mw,sh			$\nu(\text{C}=\text{C}-\text{C}=\text{O})$ SYN enol, crystal splitting
1629 m,sh	1634 m	1638 mw	1634 ms		1622 vs, vbr	$\nu(\text{C}=\text{C}-\text{C}=\text{O})$ SYN enol
1617 m,sh						$\nu(\text{C}=\text{O}) + \delta(\text{O}-\text{H})$ TS2 enol
1602 s	1605 m	1605 m	1607 ms	1604 s,br		$\nu(\text{C}=\text{O}) + \delta(\text{O}-\text{H})$ SYN enol
	1585 mw,sh	1583 mw	1585 m			$\nu(\text{C}=\text{O}) + \delta(\text{O}-\text{H})$ SYN enol, crystal splitting
	1355 w,sh	1354 w	1355 w			$\delta(\text{O}-\text{H}) + \nu(\text{C}=\text{O})$ SYN enol
	1309 mw,sh	1310 w,sh	1308 w,sh			$\nu(\text{C}-\text{C}=\text{C}) + \delta(\text{OH})$ SYN enol
			<b>1300 s, vbr</b>			luminescent band
1296 s	1296 m,br	1297 mw,br	1298 ms	1296 s,br	1307 ms	$\nu(\text{C}-\text{C}=\text{C}) + \delta(\text{O}-\text{H})$ SYN enol, crystal splitting
1200 w,br						$\delta(\text{CH})$ in-plane bending TS2 enol
1175 m	1173 mw	1174 m	1173 m	1176 mw	1172 m	$\delta(\text{CH})$ in-plane bending SYN enol
					1157 m	$\delta(\text{CH}_2)$ keto
647 s	648 s	648 ms	649 s		643 mw	out-of-plane ring bend SYN enol
635 s	642 s	642 ms	643 s	645 s		in-plane ring def. SYN enol
	624 mw			623 ms,sh	621 mw,sh	$\text{C}-\text{CH}_2-\text{C}$ bending, keto tautomer
615 w,sh					583 w	in-plane ring def. TS2 enol
555 mw	555 ms	554 m	554 ms	556 m		out-of-plane ring def. SYN enol
	534 vw			530 vw	531 mw	$\text{C}=\text{O}$ in-plane bending, out-of-phase, keto tautomer
509 w	504 m	505 mw	504 m	510 vw	513 mw	in-plane ring bend SYN enol
	413 w	413 w	412 w			in-plane ring def. SYN enol
406 vw	404 w	406 vw	403 w	406 w		in-plane ring def. TS2 enol
365 vw	358 w,br	353 w	355 w,br	372 w		in-plane ring def. SYN enol
	340 w,sh			330 w		$\text{H}_3\text{C}-\text{C}-\text{C}$ bending, keto tautomer
	235 mw	234 mw	236 mw			out-of-plane ring bend + $\gamma(\text{C}-\text{CH}_3)$ crystal splitting SYN enol
225 w			226 mw,sh	228 mw		out-of-plane ring bend + $\gamma(\text{C}-\text{CH}_3)$ SYN enol
			203 mw,sh			out-of-plane ring bend + $\gamma(\text{C}-\text{CH}_3)$ crystal splitting SYN enol
192 w	198 m	196 ms	197 m			out-of-plane ring bend + $\tau(\text{CH}_3)$ SYN enol
	174 w	170 mw	174 w			out-of-plane ring bend + $\tau(\text{CH}_3)$

						SYN enol, crystal splitting
158 w	155 w	153 w	155 w	160 m,sh		methyl group torsion SYN enol (close to C–O–H)
			113 mw,sh			lattice vibration
	101 s	101 vs	105 s			lattice vibration
	86 m,br	89 ms	90 mw			lattice vibration
	71 m	73 ms	74 m			lattice vibration
	62 vvs	63 vvs	65 vvs			coincidence of lattice vibration and methyl group torsion SYN enol (close to C $\equiv$ O)
		55 ms	55 w			lattice vibration
	48 w,sh	47 m	48 w			lattice vibration
	39 w		41 w			lattice vibration
	34 w	35 m	35 w			lattice vibration
	27 w					keto lattice phonon

<sup>a</sup> The assignment of matrix bands is based on B1LYP/6-311G(d, p) calculations for SYN and TS2 enols from ref 7. Assignment of keto bands is based on B3LYP/6-31++G(d,p) calculations,<sup>40</sup> this work.<sup>b</sup> Abbreviations. v: very, s: strong, m: medium, w: weak, as: asymmetric, sh: shoulder, br: broad.

Generally, there are no bands corresponding to the keto isomer in the spectrum of matrix-isolated acac, but there is a superposition of weaker and broader bands onto stronger and narrower bands falling at the same wavenumber (see Figure 3); such is the case of a weak band at 1687 cm<sup>-1</sup> underlying the stronger one at 1629 cm<sup>-1</sup>. We assign the band at 1687 cm<sup>-1</sup> as a quasiaromatic carbonyl stretching band in the symmetric TS2 enol, and the band at 1629 cm<sup>-1</sup> is assigned to the SYN enol. The shoulder at 1617 cm<sup>-1</sup> is assigned as the TS2 enol band, and the strong band at 1602 cm<sup>-1</sup> is assigned as belonging to the SYN enol. All 39 normal modes both for SYN and TS2 enols are active in Raman and infrared. Coussan,<sup>29</sup> Nagashima,<sup>30</sup> and Chiavassa<sup>36</sup> recorded infrared spectra of matrix-isolated acac. Nagashima's values for the argon matrix agree rather well with our reported values, and we could provide bands below 500 cm<sup>-1</sup>, neither of which were reported previously.

Matanović and Došlić<sup>7</sup> calculated the CH stretching vibration of the methyne hydrogen of SYN enol at 3101 cm<sup>-1</sup>, higher than the corresponding mode in TS2 enol at 3098 cm<sup>-1</sup> (at the anharmonic B1LYP/6-311G(d, p) level of theory). We observed two bands in the Raman matrix spectrum of acac, one at 3113 cm<sup>-1</sup> and the other at 3082 cm<sup>-1</sup>. The methyne stretching band was assigned to the band at 3008 cm<sup>-1</sup> in methylpropene,<sup>41</sup> to the 3101 cm<sup>-1</sup> band in butadiene,<sup>42</sup> while in malonaldehyde, it was assigned to the band at 2848 cm<sup>-1</sup><sup>43</sup> or reassigned to the 3060 cm<sup>-1</sup> band.<sup>44</sup> In acetylacetone, we assign the methyne CH stretching frequency of the SYN enol to the 3082 cm<sup>-1</sup> band. The band at 3113 cm<sup>-1</sup> could be a combination of the 1629 cm<sup>-1</sup> band of the SYN enol and the asymmetric methyl bending at 1464 cm<sup>-1</sup> of the same conformer.

Other bands involving the methyne group that are sensitive to the enol state are, according to ref 7, in-plane CH deformation predicted to be at 1183 cm<sup>-1</sup> for SYN enol and at 1178 cm<sup>-1</sup> for TS2 enol and out-of-plane CH deformation predicted to lie at 766 cm<sup>-1</sup> for SYN isomer and at 758

$\text{cm}^{-1}$  for TS2 enol. We observed a shoulder at  $1184 \text{ cm}^{-1}$ , a medium band at  $1175 \text{ cm}^{-1}$ , and weak bands at  $786$  and  $774 \text{ cm}^{-1}$ .

Upon careful inspection of the spectrum for the O–H stretching band, we could not confidently assign it. The weak band at  $\sim 3500 \text{ cm}^{-1}$  was also observed in a subsequent matrix-isolation experiment performed by us, but no band of acetylacetone was simultaneously observed. Therefore, the  $3500 \text{ cm}^{-1}$  band is most probably caused by remnants of methanol that was used for cleaning of the apparatus. Nagashima et al.<sup>23</sup> also observed a weak band at  $3500 \text{ cm}^{-1}$  in infrared matrix-isolation experiments and assigned it to small amounts of water interacting with acetylacetone. The bands at  $2855$  and  $2721 \text{ cm}^{-1}$  were observed in liquid and in polycrystalline solid as well and can be assigned as combinations of the SYN enol bands ( $1602 + 1250 \text{ cm}^{-1}$ ) and ( $1296 + 1435 \text{ cm}^{-1}$ ). A weak band at  $365 \text{ cm}^{-1}$  is a ring bending mode of SYN enol involving oxygen atoms.<sup>35</sup>

In conclusion, besides the SYN enol, another conformer (TS2) of acac was present in the isolate, characterized by the bands at  $1687$  and  $1617 \text{ cm}^{-1}$  and broad weak bands at  $1470$ ,  $1200$ ,  $786$ , and  $615 \text{ cm}^{-1}$ .

**Raman Spectra of Polycrystalline Acetylacetone.** Acac, which is liquid at room temperature, freezes at  $229 \text{ K}$  upon cooling and further exhibits a solid–solid phase transition at  $217 \text{ K}$  (Figure 4). Upon heating, these phase changes occur at the higher temperatures of  $254$  and  $225 \text{ K}$ . The transition at higher temperature is the freezing/melting transition, while the lower one probably involves the freezing/melting of the keto domains, as suggested by Johnson et al.<sup>20</sup> We compared Raman spectra of samples obtained by rapid cooling (spectrum at the top of Figure 5) and spectra of the annealed sample (shown at the bottom of Figure 5). The annealing procedure consisted of freezing the liquid at  $230 \text{ K}$ , heating it to  $240 \text{ K}$ , keeping it at that temperature for several hours (sometimes overnight), and then cooling down the sample to  $10 \text{ K}$ . There were no bands at  $1711$  and  $1700 \text{ cm}^{-1}$  corresponding to  $\text{C}=\text{O}$  stretching vibrations in keto isomers in the annealed samples (spectrum at the bottom of Figure 5). Other bands corresponding to keto acac in the rapidly cooled sample are the  $975 \text{ cm}^{-1}$  band (attributed to skeletal C–C stretching), the  $624 \text{ cm}^{-1}$  band (C–CH<sub>2</sub>–C bending), and the  $534 \text{ cm}^{-1}$  band (C=O in-plane bending). The positions of all observed bands are listed in Table 1 of the Supporting Material. The crystal structure of acetylacetone was determined at  $210$  and  $110 \text{ K}$  by Boese et al.<sup>19</sup> It is *Pnma* with four molecules per unit cell and molecular site symmetry  $C_{2v}$ . The number of expected optical phonons  $\Gamma_{\text{opt ph}} = 3A_g \oplus 3B_{1g} \oplus 3B_{2g} \oplus 3B_{3g} \oplus 3A_u \oplus 2B_{1u} \oplus 2B_{2u} \oplus 2B_{3u}$ . All 12 gerade phonons are Raman active, and 6 phonons of  $B_{1u}$ ,  $B_{2u}$ , and  $B_{3u}$  symmetry are infrared active. Nine low-frequency bands in the Raman spectrum of polycrystalline enol acac were assigned as lattice vibrations at  $113$ ,  $105$ ,  $90$ ,  $74$ ,  $65$ ,  $55$ ,  $48$ ,  $41$ , and  $35 \text{ cm}^{-1}$ . Phonon spectra of the annealed sample and of the sample that was rapidly cooled differ in the ratio of intensities of the  $65$  and  $105 \text{ cm}^{-1}$  phonon bands and in the appearance of the weak band at  $27 \text{ cm}^{-1}$  in the spectrum of rapidly cooled sample. Since we did not observe this band in the spectrum of annealed acac, it was assigned to a phonon from crystalline domains containing keto tautomers.

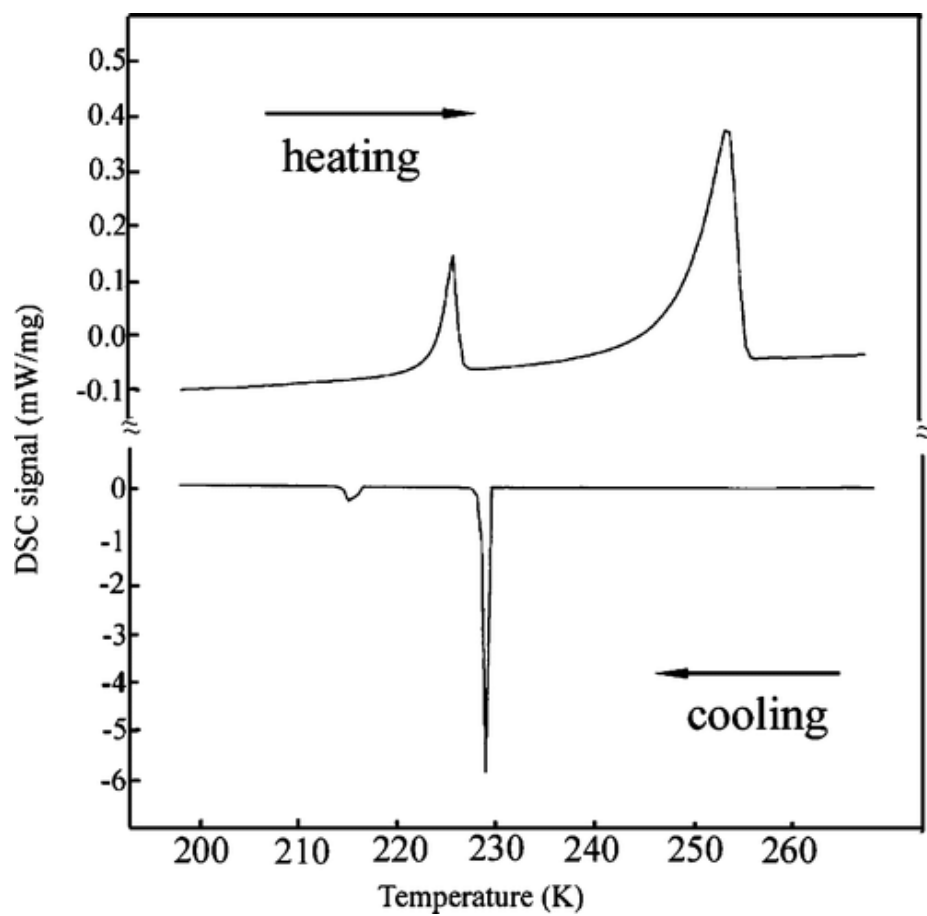
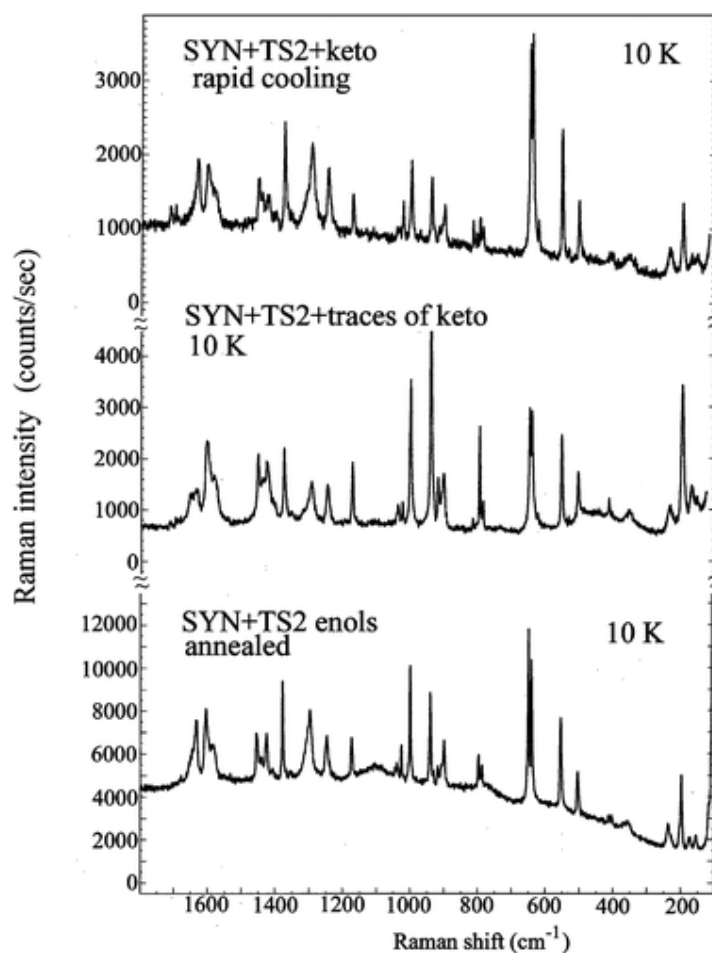


Fig 4 Differential scanning calorimetric signal of acetylacetone. The heating rate was 5 K/min, and the cooling rate was 5 K/min.



**Fig 5** Low-temperature Raman spectra of polycrystalline acetylacetone at 10 K obtained when the sample was cooled rapidly from room temperature to 10 K (spectrum at the top), when the sample was cooled to 185 K, heated above the solid–solid phase transition temperature to 230 K, and then cooled to 10 K (middle spectrum), and for the annealed sample (spectrum at the bottom) in the 100–1800  $\text{cm}^{-1}$  interval.

Among internal vibrations of acac, the lowest frequency modes are expected to be methyl torsional modes. Johnson et al.<sup>20</sup> measured methyl torsional  $0 \rightarrow 1$  transitions at 146.4 and 61.6  $\text{cm}^{-1}$  in pure enolic polycrystalline acac and attributed the higher transition to the  $\text{CH}_3$  group closer to  $\text{C-OH}$ , while the lower transition proceeds between states of the methyl group proximal to  $\text{C=O}$ . In Raman spectra of annealed crystalline acac, the weak band at 155  $\text{cm}^{-1}$  is assigned as the first torsional transition of methyl groups attached to  $\text{C-OH}$  in SYN enol form of acetylacetone molecules. The band observed at 192  $\text{cm}^{-1}$  in the matrix (Figure 3), corresponding to a mixed mode of out-of-plane ring bending and methyl torsion in SYN enol, splits in the spectrum of the annealed sample into two bands at 174 and 197  $\text{cm}^{-1}$ . In a similar manner, the band observed at 225  $\text{cm}^{-1}$  in the matrix splits into bands at 203 and 228  $\text{cm}^{-1}$  in the spectrum of the annealed sample at 10 K.

Very broad bands of medium and strong intensity accompanied all Raman spectra and are discussed in the next section. The intensity distribution among the internal modes depends on the

cooling procedure and the amount of enol conformer produced. It is often possible to observe the situation where, at 10 K, the band at  $1296\text{ cm}^{-1}$  is stronger than the band at  $1605\text{ cm}^{-1}$  (Figure 5, spectrum at the top), while in another cooling, again at 10 K, the ratio is reversed (Figure 5, spectrum in the middle).

Tayyari and Milani-Nejad<sup>35</sup> gave a thorough assignment of the SYN enol vibrations, providing also bands from the solid. They reported two bands; the one at  $1600\text{ cm}^{-1}$  was attributed to TS2 and the band at  $1630\text{ cm}^{-1}$  to the SYN conformer, while they considered the band at  $1575\text{ cm}^{-1}$  to be common to both SYN and TS2. Raman spectra in the carbonyl stretching region ( $1500\text{--}1800\text{ cm}^{-1}$ ) of polycrystalline acetylacetone and matrix-isolated acac are compared in Figure 6. Whereas at 85 K there is only one band at  $1630\text{ cm}^{-1}$  in the polycrystalline annealed sample (spectrum at the top), at 10 K, there is also a shoulder at  $1652\text{ cm}^{-1}$  (spectrum in the middle), besides the other two bands at 1600 and  $1585\text{ cm}^{-1}$ . All of these bands are attributed to two internal SYN enol modes, which split into four modes in the crystal (see Table 1 for mode description).

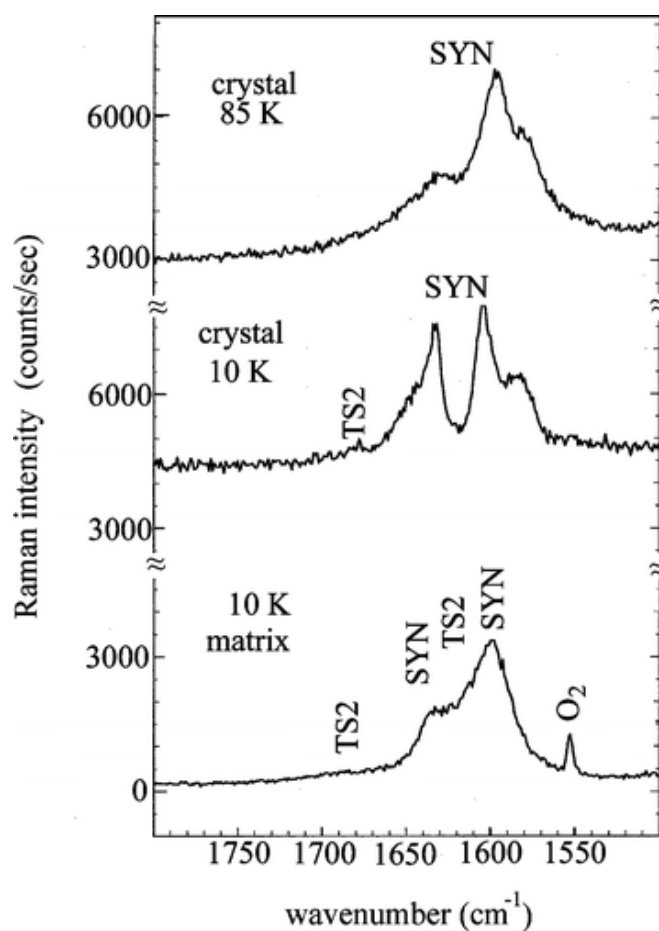
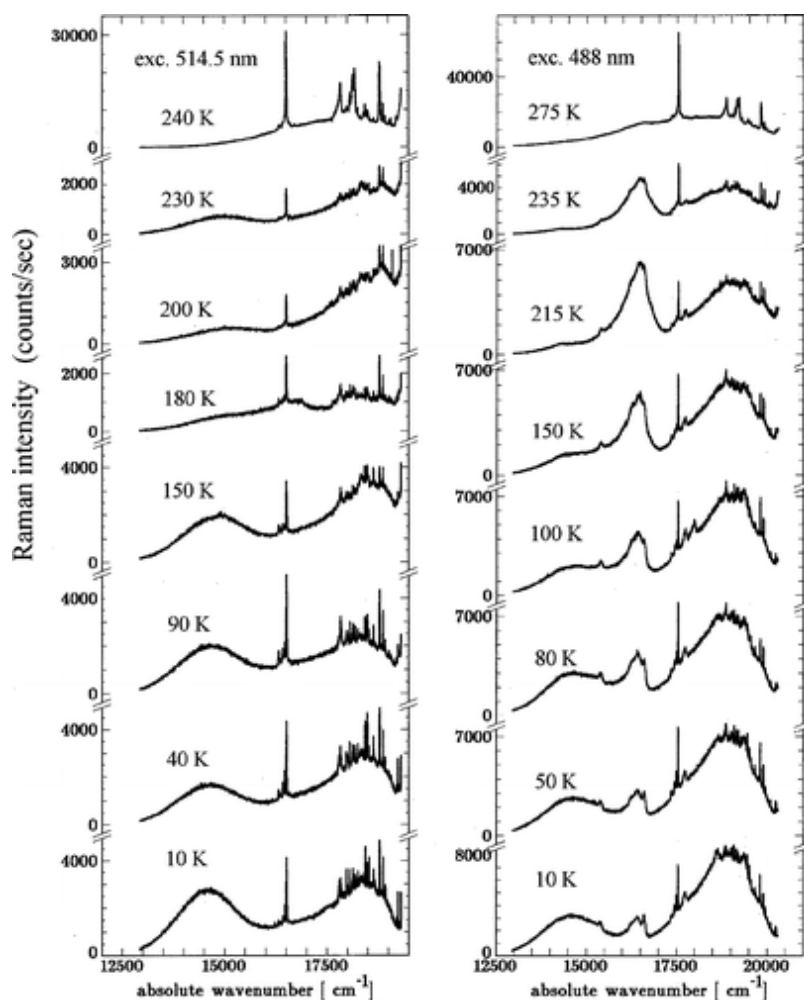


Fig 6 Comparison of Raman spectra of annealed polycrystalline acetylacetone at 85 K (spectrum at the top), at 10 K (middle spectrum), and with the spectrum of matrix-isolated acetylacetone at 10 K (spectrum at the bottom) ( $1500\text{--}1800\text{ cm}^{-1}$ ). Bands in the crystal belong to SYN enol, except a very weak band at  $1683\text{ cm}^{-1}$  observed at 10 K and attributed to TS2 enol.

**Luminescence in Polycrystalline Acetylacetone.** Luminescence bands are reported to appear together with Raman spectra of organic solutions<sup>45</sup> in superconductors<sup>46</sup> and conjugated polymers.<sup>47</sup> Usually, vibrational spectroscopists attribute the term luminescence to bands which appear in Raman spectra at different wavenumbers when different laser lines are used for excitation (their Raman shift varies) but are at the same absolute wavenumbers. Figure 7 shows the temperature-dependent Raman spectra of acac that were obtained when the green or blue laser line served as the excitation source. There are more bands when the blue line is used, and their band centers shift a little.



**Fig 7** Temperature-dependent Raman spectra of acetylacetone displaying strong broad luminescence bands corresponding to frozen relaxation from higher energy isomers (see text). The excitation wavelengths were 514.5 nm ( $19436\text{ cm}^{-1}$ ) and 488 nm ( $20458\text{ cm}^{-1}$ ).

In the literature,<sup>27-34</sup> there are several studies reporting on the UV photoisomerization of acetylacetone and of experiments performed using infrared radiation for conversions of one matrix-trapped isomer into the other. Here, we report photoisomerization that is going on in the visible part of the spectrum when the sample is solid at low temperature. The fact that the acac is

solid at low temperature has two important consequences. First, if the sample is liquid, no absorption in the 2.2–2.5 eV interval can take place because the electronic states of molecules in liquid resemble those of free molecules, and in that energy interval, only the triplet  $T_2$  state is predicted to exist (or a series of triple states for different isomers).<sup>8,29-31</sup> We also recorded some UV–vis absorbance spectra of liquid acac, and there were no absorption bands in the 450–550 nm interval for liquid. Second, photons cannot be emitted if molecules make transitions from pure triplet states to the ground singlet state (spin zero); therefore, the electronic states to which acac molecules are excited and from which they decay into the ground state must have partial singlet character in the crystal. The broad bands that we report in Figure 7 (the laser line is green, 514.5 nm, energy 2.41 eV) are not at the same wavenumbers as those which appear when the blue laser line (at 488.8 nm, energy 2.53 eV) is used. The assignment of the band centers given in Table 2 is approximate because we compared the position of the band centers with the predicted energy difference for each isomer  $E_{\text{laser}} - E_{\text{isomer}}$ .<sup>8,10,30</sup>

**Table 2 Observed Broad Bands Underlying Low-Temperature Raman Spectra of Acetylacetone**

excitation $\lambda_0 = 514.5 \text{ nm } \nu_{\sim 0} = 19436 \text{ cm}^{-1}$				Excitation $\lambda_0 = 488.8 \text{ nm } \nu_{\sim 0} = 20458 \text{ cm}^{-1}$			
$T$ (K)	$\nu_{\sim R}$ ( $\text{cm}^{-1}$ )	$\nu_{\sim 0} - \nu_{\sim R}$ ( $\text{cm}^{-1}$ )	AcAc isomer giving origin to the band	$T$ (K)	$\nu_{\sim R}$ ( $\text{cm}^{-1}$ )	$\nu_{\sim 0} - \nu_{\sim R}$ ( $\text{cm}^{-1}$ )	AcAc isomer giving origin to the band
230	4635	14800	CTC,CTT	235	6208	14250	CCT
	785	18650	TS1 enol + keto		3958	16500	CTC,CTT,TCC
200	4435	15000	CTC,CTT		1458	19000	TS1 enol + keto
	835	18600	TS1 enol + keto	215	6158	14300	CCT
180	4200	15236	CTC,CTT		3958	16500	CTC,CTT,TCC
	2735	16700	transition state		1490	18968	TS1 enol + keto
	1035	18400	TS1 enol + keto	150	5758	14700	CCT
150	4635	14800	CTC,CTT,TCC		4008	16450	CTC,CTT,TCC
	985	18450	TS1 enol + keto		1458	19000	TS1 enol + keto
90	4735	14700	CTC,CTT,TCC	100	5758	14700	CCT
	1085	18350	TS1 enol + keto		4008	16450	CTC,CTT,TCC
					1458	19000	TS1 enol + keto
40	4735	14700	CTC,CTT,TCC	80	5758	14700	CCT
	1035	18400	TS1 enol + keto		4008	16450	CTC,CTT,TCC
					1558	18900	TS1 enol + keto
10	4835	14600	CTC,CTT,TCC	50	5858	14600	CCT
	1085	18350	TS1 enol + keto		4058	16400	CTC,CTT,TCC
					1558	18900	TS1 enol + keto
				10	5858	14600	CT
					4058	16400	CTC,CTT,TCC
					1558	18900	TS1 enol + keto

## Discussion

Among systems displaying keto–enol tautomerism, such as 1-hydroxyanthraquinone<sup>48</sup> or 2-(2'-hydroxyphenyl)benzoxazole,<sup>49</sup> enol and keto singlet and triplet states are close in energy, and upon excitation, a number of relaxation pathways are possible. A similar situation is found in acetylacetone, whose excited electronic states were studied by Chen et al.,<sup>8</sup> Nakanishi et al.,<sup>27</sup> Coussan et al.,<sup>28</sup> Nagashima et al.,<sup>30</sup> and Upadhyaya et al.,<sup>31</sup> among others. The strong UV band appearing at 266 nm in the absorption spectra corresponds to the  $S_0 \rightarrow S_2$  transition. The  $S_2$  state decays into lower  $S_1$ ,  $T_2$ , and  $T_1$  states, which decay further into ground states of different acac isomers.<sup>27-34</sup> The notation used to describe the isomers consists of three capital letters CCC, CTC, and so forth. The first letter refers to the conformation with respect to rotation around the carbon–carbon single bond in the ring, the second letter describes conformation with respect to rotation around the double carbon bond, and the third letter refers to conformation with respect to rotation around the carbon–hydroxyl oxygen bond. Absorption selection rules for photons forbid singlet-to-triplet transitions, but it is known that, in the solid state, the excited states are not pure singlet or triplet states.<sup>47</sup> Figure 8 shows an energy level diagram depicting data from Matanović and Došlić,<sup>10</sup> Nagashima et al.,<sup>30</sup> and Chen et al.<sup>8</sup> In the interest of clarity, not all transition triplet states listed in ref 8 are shown. One can see that, in the region of our green laser excitation ( $19436\text{ cm}^{-1}$ ), the enol triplet state of the free acac molecule  $E(T_1)$  is predicted at  $19845\text{ cm}^{-1}$ ,<sup>8</sup> while around the energy of the blue argon ion laser line ( $20458\text{ cm}^{-1}$ ), three states are predicted at  $20405$ , (CTT( $T_1$ )),  $20440$  (CCT( $T_1$ )), and  $20545\text{ cm}^{-1}$  (TCC( $T_1$ )).<sup>8</sup> Because electronic states in the solid have bandwidths on the order of  $1600\text{ cm}^{-1}$ ,<sup>50</sup> these states are all accessible with our laser excitation. In Table 2, we give the tentative assignment of the broad bands observed in polycrystalline acac shown in Figure 7. Three isomers have their energy approximately  $4000\text{--}5000\text{ cm}^{-1}$  above the ground state of the CCC isomer. They are CTC, CTT, and TCC isomers, and the bands that correspond to them occur in the  $14200\text{--}14800\text{ cm}^{-1}$  interval when the green laser line is used ( $514.5\text{ nm}$ ) and in the  $16400\text{--}16600\text{ cm}^{-1}$  interval when the  $488\text{ nm}$  excitation is used. The huge intensity difference observed in the case of the blue line is caused by a preresonance condition; the energy of the excited mixed singlet–triplet bands is dependent on temperature in such a manner that, at  $215\text{ K}$ , the laser photons are closer in energy to the excited singlet/triplet band of the CTC, CTT, and TCC isomers. At  $100\text{ K}$  and below, the excited singlet/triplet states of the keto isomer and TS1 enol are closer to the energy of incoming photons. Upon excitation, molecules relax to the ground isomer states, whose populations reflect this.

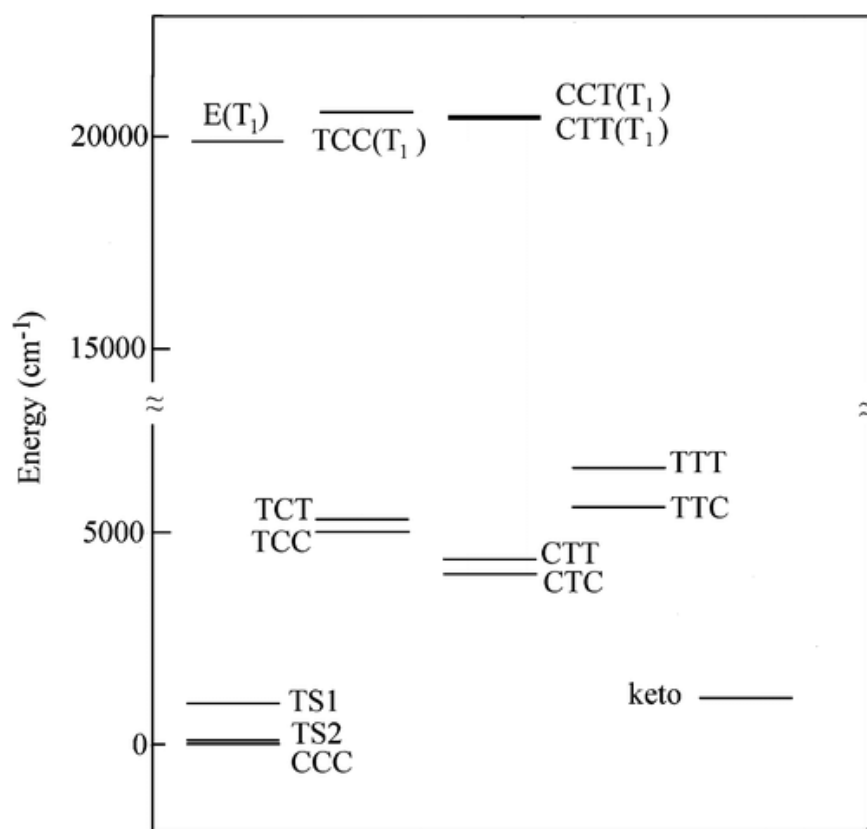


Fig 8 Energy level diagram of acetylacetone ground and excited states based on predicted values for TS1 and TS2,<sup>10</sup> E(T<sub>1</sub>), TCC(T<sub>1</sub>), CCT(T<sub>1</sub>), and CTT(T<sub>1</sub>)<sup>8</sup> and the rest from ref 30. Not all states are shown; please see references mentioned for a more complete list.

In matrix-isolation experiments, no luminescence bands were observed because of the weak interactions between molecules. In polycrystalline solid, on the other hand, the intermolecular interaction caused changes in the nature of the excited electronic states of acac from the pure triplet to mixtures of singlet and triplet states.

## Conclusion

Light-scattering experiments on acetylacetone at low temperatures display a number of strong broad bands appearing beneath the Raman spectra of the solid. These results are interpreted as transitions from molecules excited to higher states to various isomers in the ground electronic state. Laser photons of energies 19436 and 20458 cm<sup>-1</sup> excite acac in the region where a number of excited triplet states are predicted for the free acetylacetone molecule. Since singlet-to-triplet photon absorption transitions are forbidden, we conclude that states existing in solid acac have mixed singlet/triplet character. Their decay results in population of different isomer states, which are not vibrationally resolved, except for the lowest isomers, SYN enol, the TS2 transition state, and the keto form, which can be detected in solid Raman spectra.

The molecular conformation of matrix-isolated acetylacetone is dominantly SYN enol. Nevertheless, bands corresponding to the enol conformer, with symmetrically placed methyl groups (TS2 enol), are also observed.

## Acknowledgment

This work was made possible by the Grants 0098019, 0098022, and 0125019 of the Ministry of Science, Technology and Sport of the Republic of Croatia. Thanks are due to Mr. David M. Smith for kindly reading the manuscript.

## Supporting Information Available

Observed Raman and infrared bands, calculated unscaled frequencies, and Raman spectra. This material is available free of charge via the Internet at <http://pubs.acs.org>.

## References

- (1) Emsley, J. *Struct. Bonding* **1984**, *57*, 147.
- (2) Imao, T.; Noma, N.; Ito, S. *J. Sol-Gel Sci. Technol.* **2006**, *38*, 197.
- (3) Tsaryuk, V.; Zolin, V.; Legendziewicz, J.; Szostak, R.; Sokolnicki, J. *Spectrochim. Acta, Part A* **2005**, *61*, 185.
- (4) Zhang, R.-J.; Yang, K.-Z.; Yu, A.-C.; Zhao, X.-S. *Thin Solid Films* **2000**, *363*, 275.
- (5) Cohen, B.; Weiss, S. *J. Phys. Chem.* **1984**, *88*, 3159.
- (6) Emsley, J.; Freeman, N. J. *J. Mol. Struct.* **1987**, *161*, 193.
- (7) Matanovic', I.; Dos'lic', N. *Int. J. Quantum Chem.* **2006**, *106*, 1367.
- (8) Chen, X.-B.; Fang, W.-H.; Phillips, D. L. *J. Phys. Chem. A* **2006**, *110*, 4434.
- (9) Cabral do Couto, P.; Costa Cabral, B. J.; Martinho Simoes, J. A. *Chem. Phys. Lett.* **2006**, *419*, 486.
- (10) Matanovic', I.; Dos'lic', N. *J. Phys. Chem. A* **2005**, *109*, 4185.
- (11) Campomanes, P.; Menendez, M. I.; Sordo, T. L. *J. Mol. Struct.: THEOCHEM* **2005**, *713*, 59.
- (12) Matanovic', I.; Dos'lic', N.; Mihalic', Z. *Chem. Phys.* **2004**, *306*, 201.
- (13) Szilnev, V. V.; Lapshina, S. B.; Girichev, G. V. *J. Struct. Chem.* **2002**, *43*, 47.
- (14) Mavri, J.; Grdadolnik, J. *J. Phys. Chem. A* **2001**, *105*, 2039.
- (15) Mavri, J.; Grdadolnik, J. *J. Phys. Chem. A* **2001**, *105*, 2045.
- (16) Sharafeddin, O. A.; Hinsen, K.; Carrington, T., Jr.; Roux, B. *J. Comput. Chem.* **1997**, *18*, 1760.
- (17) Dannenberg, J. J.; Rios, R. *J. Phys. Chem. A* **1994**, *98*, 6714.
- (18) Gromak, V. V. *J. Mol. Struct.: THEOCHEM* **2005**, *726*, 213.
- (19) Boese, R.; Antipin, M. Yu.; Bla"ser, D.; Lyssenko, K. A. *J. Phys. Chem. B* **1998**, *102*, 8654.

- (20) Johnson, M. R.; Jones, N. H.; Geis, A.; Horsewill, A. J.; Trommsdorff, H. P. *J. Chem. Phys.* **2002**, *116*, 5694.
- (21) Caminati, W.; Grabow, J.-U. *J. Am. Chem. Soc.* **2006**, *128*, 854.
- (22) Lowrey, A. H.; George, C.; D'Antonio, P.; Karle, J. *J. Am. Chem. Soc.* **1971**, *93*, 6399.
- (23) Ijima, K.; Ohnogi, A.; Shibata, S. *J. Mol. Struct.* **1987**, *156*, 111.
- (24) Srinivasan, R.; Feenstra, J.-S.; Park, S. T.; Xu, S.; Zewail, A. H. *J. Am. Chem. Soc.* **2004**, *126*, 2266.
- (25) Camerman, A.; Mastropaolo, D.; Camerman, N. *J. Am. Chem. Soc.* **1983**, *105*, 1584.
- (26) Veierov, D.; Bercovici, T.; Fischer, E.; Mazur, Y.; Yogev, A. *J. Am. Chem. Soc.* **1973**, *95*, 8173.
- (27) Nakanishi, H.; Morita, H.; Nagakura, S. *Bull. Chem. Soc. Jpn.* **1977**, *50*, 2255.
- (28) Coussan, S.; Ferro, Y.; Trivella, A.; Rajzmann, M.; Roubin, P.; Wieczorek, R.; Manca, C.; Piecuch, P.; Kowalski, K.; Wloch, M.; Kucharski, S. A.; Musial, M. *J. Phys. Chem. A* **2006**, *110*, 3920.
- (29) Coussan, S.; Manca, C.; Ferro, Y.; Roubin, P. *Chem. Phys. Lett.* **2003**, *370*, 118.
- (30) Nagashima, N.; Kudoh, S.; Takayanagi, M.; Nakata, M. *J. Phys. Chem. A* **2001**, *105*, 10832.
- (31) Upadhyaya, H. P.; Kumar, A.; Naik, P. D. *J. Chem. Phys.* **2003**, *118*, 2590.
- (32) Minoura, Y.; Nagashima, N.; Kudoh, S.; Nakata, M. *J. Phys. Chem. A* **2004**, *108*, 2353.
- (33) Walzl, K. N.; Xavier, I. M., Jr.; Kuppermann, A. *J. Chem. Phys.* **1987**, *86*, 6701.
- (34) Schweig, A.; Vermeer, H.; Weidner, U. *Chem. Phys. Lett.* **1974**, *26*, 229.
- (35) Tayyari, S. F.; Milani-Nejad, F. *Spectrochim. Acta, Part A* **2000**, *56*, 2679.
- (36) Chiavassa, T.; Verlaque, P.; Pizzala, L.; Roubin, P. *Spectrochim. Acta, Part A* **1994**, *50*, 343.
- (37) Tayyari, S. F.; Zeegers-Huyskens, Th.; Wood, J. L. *Spectrochim. Acta, Part A* **1979**, *35*, 1265.
- (38) Tayyari, S. F.; Zeegers-Huyskens, Th.; Wood, J. L. *Spectrochim. Acta, Part A* **1979**, *35*, 1289.
- (39) Ogoshi, H.; Nakamoto, K. *J. Chem. Phys.* **1966**, *45*, 3113.
- (40) Frisch, M. J.; Trucks, G. W.; Schlegel, H. B.; Scuseria, G. E.; Robb, M. A.; Cheeseman, J. R.; Montgomery, J. A., Jr.; Vreven, T.; Kudin, K. N.; Burant, J. C.; Millam, J. M.; Iyengar, S. S.; Tomasi, J.; Barone, V.; Mennucci, B.; Cossi, M.; Scalmani, G.; Rega, N.; Petersson, G. A.; Nakatsuji, H.; Hada, M.; Ehara, M.; Toyota, K.; Fukuda, R.; Hasegawa, J.; Ishida, M.; Nakajima, T.; Honda, Y.; Kitao, O.; Nakai, H.; Klene, M.; Li, X.; Knox, J. E.; Hratchian, H. P.; Cross, J. B.; Bakken, V.; Adamo, C.; Jaramillo, J.; Gomperts, R.; Stratmann, R. E.; Yazyev, O.; Austin, A. J.; Cammi, R.; Pomelli, C.; Ochterski, J. W.; Ayala, P. Y.; Morokuma, K.; Voth, G. A.; Salvador, P.; Dannenberg, J. J.; Zakrzewski, V. G.; Dapprich, S.; Daniels, A. D.; Strain, M. C.; Farkas, O.; Malick, D. K.; Rabuck, A. D.; Raghavachari, K.; Foresman, J. B.; Ortiz, J. V.; Cui, Q.; Baboul, A. G.; Clifford, S.; Cioslowski, J.; Stefanov, B. B.; Liu, G.; Liashenko, A.; Piskorz, P.; Komaromi, I.; Martin, R. L.; Fox, D. J.; Keith, T.; Al-Laham, M.

- A.; Peng, C. Y.; Nanayakkara, A.; Challacombe, M.; Gill, P. M. W.; Johnson, B.; Chen, W.; Wong, M. W.; Gonzalez, C.; Pople, J. A. *Gaussian 03*, revision C.02; Gaussian, Inc.: Wallingford, CT, 2004 (41) Radiszewski, J. G.; Downing, J. W.; Gudipati, M. S.; Balaji, V.; Thulstrup, E. W.; Michl, J. *J. Am. Chem. Soc.* **1996**, *118*, 10275.
- (42) Wilson, E. B.; Smith, Z. *J. Mol. Spectrosc.* **1982**, *94*, 399.
- (43) Wilson, E. B.; Smith, Z.; Duerst, R. *Spectrochim. Acta, Part A* **1983**, *39*, 1117.
- (44) Tayyari, S. F.; Milani-Nejad, F. *Spectrochim. Acta, Part A* **1998**, *54*, 255.
- (45) Nakamura, R.; Yamamoto, S.; Nakahara, J. *J. Chem. Phys.* **2002**, *117*, 238.
- (46) Kuroe, H.; Kaneko, T.; Sekine, T.; Sarmago, R. V.; Koide, N.; Masuda, T.; Tsukada, I.; Uchinokura, K. *Physica B* **2000**, *284-288*, 1643.
- (47) Woo, H. S.; Graham, S. C.; Halliday, D. A.; Bradley, D. D. C.; Friend, R. H. *Phys. Rev. B* **1992**, *46*, 7379.
- (48) Cho, D. W.; Kim, S. H.; Yoon, M.; Jeoung, S. C. *Chem. Phys. Lett.* **2004**, *391*, 314.
- (49) Walla, P.; Nickel, B. *Chem. Phys.* **2005**, *312*, 177.
- (50) Petelenz, P.; Slawik, M.; Yokoi, K.; Zgierski, M. Z. *J. Chem. Phys.* **1996**, *105*, 4427.